

Alignment of the CMS Silicon Tracker – and how to improve detectors in the future

Claus Kleinwort^a, Frank Meier^{b,1,*}

^aDESY Deutsches Elektronen-Synchrotron, Notkestraße 85, 22607 Hamburg, Germany

^bPaul Scherrer Institut, OFLC/009, 5232 Villigen, Switzerland

Abstract

The complex system of the CMS all-silicon Tracker, with 15 148 silicon strip and 1440 silicon pixel modules, requires sophisticated alignment procedures. In order to achieve an optimal track-parameter resolution, the position and orientation of its modules need to be determined with a precision of few micrometers. The alignment of pixels modules is crucial for the analyses requiring a precise vertex reconstruction. The aligned geometry is based on the analysis of several million reconstructed tracks recorded during the commissioning of the CMS experiment, both with cosmic rays and with the first proton-proton collisions. Statistical precision of the alignment of the module with respect to the particle trajectories to less than 10 microns has been achieved. The results have been validated by several data-driven studies (track fit self-consistency, track residuals in overlapping module regions, and track parameter resolution) and compared with predictions obtained from a detailed detector simulation.

Recent developments include the determination of sensor bow and displacements between sensors of composite modules.

Thoughts on improving future detectors with respect to alignment are given.

Keywords: Pixel detector, CMS, track-based alignment, Millepede-II, Broken Lines

1. Introduction

The all-silicon inner tracker of the CMS detector at CERN consists of 15 148 silicon strip and 1440 silicon pixel modules in a barrel-and-endcap configuration[1]. Its main purpose is to determine track parameters of charged particles produced in proton-proton and heavy ion collisions. The parameters to be delivered per track are the charge-signed curvature κ (i.e. inverse transverse momentum), the impact parameters in the transverse plane and along the beam axis, d_{xy} , d_z respectively, and the polar angles θ and ϕ . The intrinsic hit resolutions of the detector modules are of the order of a few tens of microns, depending on module type and location. In order to determine the track parameters with high precision, the positions of the sensor modules need to be known better than their resolution. Alignment using large amounts of track data (typically several millions) is one approach to fulfill this requirement.

2. Track-based alignment

The use of tracks to align a tracking detector is possible under the assumption, that tracks may be described using a limited and sufficient number of parameters in an appropriate way to predict their paths. Misalignment leads to a systematic distortion of the measurements per module which can be determined using sufficiently large number of tracks and their hit signals.

In CMS, the alignment software consists of two independent algorithms, tools for the study of random and systematic misalignments and an extensive collection of tools to monitor and visualize the performance and geometry of the detector. They use track data from collision or cosmic ray muons, both as simulated and real data.

Track-based alignment relies on a suitable description of the track and its propagation through matter, as defined by the chosen detector geometry. It can be formulated as a *linear least squares problem* where the following expression needs to be minimized:

$$\chi^2(\mathbf{p}, \mathbf{q}) = \sum_j^{\text{tracks}} \sum_i^{\text{hits}} \mathbf{r}_{ij}^T(\mathbf{p}, \mathbf{q}_j) \mathbf{V}_{ij}^{-1} \mathbf{r}_{ij}(\mathbf{p}, \mathbf{q}_j) \quad (1)$$

where \mathbf{r}_{ij} is the residual vector containing all residuals from the tracks used and their hits, defined as

$$\mathbf{r}_{ij} = \text{track-model prediction} - \text{measured hit.}$$

The residuals are a function of \mathbf{p} , the vector containing all alignment parameters describing the actual geometry and \mathbf{q}_j , the track parameters of the j^{th} track. \mathbf{V}_{ij}^{-1} is the inverse covariance matrix containing all information on the measurement precision and their correlations. Position and orientation of the detector modules contribute 6 or 5 degrees of freedom for silicon pixel and strip detectors, respectively. This defines the size of a sub-vector of \mathbf{p} describing one sensor.

Using a sufficiently large sample of tracks, equation (1) and its summands follow a χ^2 distribution for a corresponding num-

*Both authors on behalf of the CMS Collaboration
Email addresses: claus.kleinwort@desy.de (Claus Kleinwort),
frank.meier@psi.ch (Frank Meier)

¹Corresponding author

47 *ber of degrees of freedom* (ndof), obeying

$$\left\langle \frac{\chi^2(\mathbf{p}, \mathbf{q})}{\text{ndof}} \right\rangle = 1 \quad \langle \text{prob}(\chi^2, \text{ndof}) \rangle = \frac{1}{2} \quad (2)$$

48 In the case of a detector of the size as in CMS, alignment al-
49 gorithms need to reduce their complexity while preserving their
50 focus on solving the problem for two reasons: 1) The total num-
51 ber of parameters \mathbf{p} and \mathbf{q} gets large. Aligning 16 000 mod-
52 ules for position and angle leads to about 60 000 parameters in
53 \mathbf{p} . The developments described in this paper will increase this
54 number. 2) The results should be delivered within a reasonable
55 time-frame. The two approaches in CMS to manage this are as
56 follows:

57 *Local algorithm.* This algorithm reduces the workload by
58 aligning the modules independently ignoring correlations at
59 first glance. Each module is forced to the position predicted
60 by the track hits from the other (unaligned) modules. Intrinsic-
61 ally, it uses the track parametrization and propagation from the
62 CMS tracking, which takes all necessary effects of the magnetic
63 field and material interactions into account. This approach re-
64 covers correlations between modules by iterating over the same
65 event sample several times. At each iteration the tracks are re-
66 fitted using the alignment corrections obtained in the previous
67 iteration. Eventually the procedure yields converged alignment
68 constants. This algorithm is known as the *HIP-algorithm*[2, 3].

69 *Global algorithm.* This approach reduces the complexity by
70 the observation that it is sufficient to solve for the module pa-
71 rameters \mathbf{p} alone. This can be achieved by requiring indepen-
72 dent measurements and the use of block-matrix theorems. This
73 is implemented in the *Millepede-II* alignment algorithm[4]. As
74 this presentation focuses on some recent results produced using
75 this algorithm, a more detailed description follows now.

76 2.1. Millepede-II

77 To accommodate for nonlinearities introduced by the track
78 parametrization (\mathbf{q}) and by the module parameters (\mathbf{p}), equation
79 (1) needs to be linearized:

$$\chi^2(\mathbf{p}, \mathbf{q}) = \sum_j^{\text{tracks}} \sum_i^{\text{hits}} \frac{1}{\sigma_{ij}^2} \left(\mathbf{m}_{ij} - \mathbf{f}_{ij}(\mathbf{p}_0, \mathbf{q}_{j0}) - \frac{\partial \mathbf{f}_{ij}}{\partial \mathbf{p}} \Delta \mathbf{p} - \frac{\partial \mathbf{f}_{ij}}{\partial \mathbf{q}_j} \Delta \mathbf{q}_j \right)^2 \quad (3)$$

80 where \mathbf{f}_{ij} is the hit position predicted by the track model from
81 track reconstruction and \mathbf{m}_{ij} is the measured hit position. As-
82 suming uncorrelated measurements allows to replace the in-
83 verse covariance matrix by $\frac{1}{\sigma_{ij}^2}$ with σ_{ij} the Gaussian error of
84 the measured hit position.

85 The track model used in CMS is the Kálmán filter description
86 including proper description of material effects[5] and the prop-
87 agation in the magnetic field[6]. By design, it is a sequential fit
88 and cannot produce the covariance matrix for all track parame-
89 ters. In principle, it is possible to gain this information for all
90 tracks a posteriori, but the *Broken Lines* approach as described

91 in [7] can be implemented more efficient and is equivalent to
92 the Kálmán approach. A brief description follows:

93 A charged particle traversing material experiences *multiple*
94 *scattering*, mainly due to Coulomb interaction with the elec-
95 trons in the atoms, resulting in a spatial shift and a change of the
96 particle direction after leaving the material compared to propa-
97 gation in vacuum. The mean of the deflection angle due to this
98 effect is $\langle \beta \rangle = 0$. The distribution of the deflection angles can
99 be approximated within certain limits as a Gaussian standard
100 deviation $\sigma(\beta)$ by the following formula[8]:

$$\sigma(\beta) = \frac{13.6 \text{ MeV}}{vp} z \sqrt{x/X_0} [1 + 0.038 \ln(x/X_0)] \quad (4)$$

101 where $v = \beta c$ (here β as rel. velocity factor) is the velocity of the
102 particle, p its momentum and z the charge. x/X_0 is the thickness
103 of the traversed medium in units of radiation lengths.

104 Equation (4) takes into account all material traversed by
105 the particle for the full trajectory. Care has to be taken dur-
106 ing propagation, as simple summing up contributions of sub-
107 paths leads to too large estimates of $\sigma(\beta)$ by the ln-term in the
108 bracket (details in reference). It is standard procedure to treat
109 a “thick” scatterer (material with a finite thickness) as two in-
110 finitely “thin” scatterers with same mean and sigma spaced by
111 $1/\sqrt{3}$ of the length of the “thick” scatterer. In a tracking de-
112 tector as in CMS, most of the material is concentrated at layers
113 coinciding with the detector modules. They consist of matter
114 in which the sensor interaction takes place and of non-sensing
115 matter like support structures, cabling and cooling pipes. So the
116 two “thin” scatterers coincide in the detector planes.

117 To determine the momentum of the charged particles’ tracks,
118 a strong and sufficiently homogeneous magnetic field of 3.8 T is
119 present in the tracker. This can be taken into account by adjust-
120 ing the expectation value of the scattering angle of a propagated
121 particle (β) ($=0$ without B-field) to the value defined by the ac-
122 cumulated Lorentz force while propagating through the field.

123 Taking all this into account, the sum over all hits of one track
124 in (3) becomes

$$\chi^2(\kappa, \mathbf{u}) = \sum_{i=1}^{n_{\text{meas}}} (\mathbf{m}_i - \mathbf{P}_i \mathbf{u}_{\text{int},i})^T \mathbf{V}_{\text{meas},i}^{-1} (\mathbf{m}_i - \mathbf{P}_i \mathbf{u}_{\text{int},i}) + \sum_{i=2}^{n_{\text{scat}}-1} \boldsymbol{\beta}_i(\kappa, \mathbf{u})^T \mathbf{V}_{\boldsymbol{\beta},i}^{-1} \boldsymbol{\beta}_i(\kappa, \mathbf{u}) \quad (5)$$

125 where $\boldsymbol{\beta}_i$ is a vector of additional parameters of the track at
126 every scatterer to account for the deflection angles. κ is the
127 charge-signed curvature, $\mathbf{u} = (\mathbf{u}_1, \dots, \mathbf{u}_{n_{\text{scat}}})$ describe the hit po-
128 sition in some local frame of the sensor and the projection ma-
129 trix \mathbf{P}_i translates between the track frame and the local frame.
130 The sums run over n_{meas} recorded hits and n_{scat} scatterers along
131 one track, normally $n_{\text{meas}} < n_{\text{scat}}$ as the detector is neither fully
132 hermetic nor efficient.

133 Solving for the minimum of eq. (5) leads to a bordered band
134 matrix: One $\boldsymbol{\beta}_i$ depends on the hit and its neighbours only, lead-
135 ing to a band matrix structure of band width m . The border
136 b in the matrix comes from κ , which is connected to every hit

137 along a track. This structure allows for fast solution and de-188
 138 termination of the covariance matrix using root-free Cholesky-189
 139 decomposition with a numeric complexity of $O(n^2(m+b))$, com-190
 140 pared to $O(n^3)$ for inversion. This is needed for the refit internal-191
 141 to MillePede for single tracks.

142 All this leads to a track description equivalent to the Kálmán
 143 filter model, as shown in [9]. It has the advantage, that the in-
 144 verse covariance matrix for one track is a bordered band matrix,
 145 which can be inverted by root-free Cholesky decomposition, a
 146 faster approach than inversion.

147 3. More detailed surface description

148 Millepede-II uses an internal track refit as part of its proce-
 149 dure. Careful studies of its results as a function of track param-
 150 eters have been carried out. Deviations were found while investig-
 151 ating tracks from cosmic ray muons. A strong dependence
 152 of the $\langle\chi^2\rangle$ on the distance of closest approach d_0 to the beam-
 153 line (corresponding to track parameter d_{xy}) was found. This can
 154 be seen in figure 2, curve for *flat module*. Several hypotheses
 155 for the source of this effect have been analyzed. It is an intrinsic
 156 property of cosmic rays to have $d_0 \gg 0$ in general, which
 157 translates to a large incident angle on rectangular modules in
 158 the barrel-shaped part of the detector. For example, whenever
 159 d_0 is slightly smaller than the radius of a barrel layer, the track,
 160 angle becomes especially large, making the hit position highly,
 161 sensitive to deviations from an ideal flat rectangle. In the end-
 162 cap parts of the detector, the incident angle of the cosmic ray
 163 muons is always large, independent of d_0 .

164 To take deviations from a flat surface into account, the sur-
 165 face has been expanded in terms of two-dimensional Legendre,
 166 polynomials:

$$w(u, v) = \sum_{i=0}^N \sum_{j=0}^i c_{ij} L_j(u) L_{i-j}(v) \quad (6)$$

167 where $w(u, v)$ is the deviation from a plane at the origin of a
 168 right-handed local cartesian coordinate system (uvw) in w di-
 169 rection as function of u, v . N is the maximal order of the Leg-
 170 endre polynomials. For $N \rightarrow \infty$ every possible surface may
 171 be described. c_{ij} are the orthogonal coefficients and $L_i(x)$ the
 172 Legendre polynomial of i -th order.

173 $N = 1$ corresponds to the flat module assumption as used
 174 prior to this extension (except for translations in u, v and rota-
 175 tions around w , which are not covered by (6) and need the same
 176 treatment as before). $N = 2$ introduces three additional param-
 177 eters per module: c_{20}, c_{11} and c_{02} . The first and last can be trans-
 178 lated by choosing a proper normalization to sagittae. c_{11} de-
 179 scribes a mix-term similar to a twist. Extending the alignment
 180 to these parameters lead to the curve for *flat module* in figure
 181 2. Figure 1(a) clearly shows how the residuals as a function of
 182 the hit position along strip modules recover to an expected flat
 183 distribution when taking the bowing of the sensors into account.

184 The sensors at larger radii of the barrel and endcaps are com-
 185 posite modules, i.e. two sensors are mounted in one module
 186 frame and daisy chained to one readout electronic block. Do-
 187 ing the same graph for composite modules (figure 1(b)) clearly

shows another deviation from the expected curve. This is at-
 tributed to angles between the sensors. This has been imple-
 mented as well by treating the individual sensors as separate
 entities, which lead to the remaining curves in figure 2.

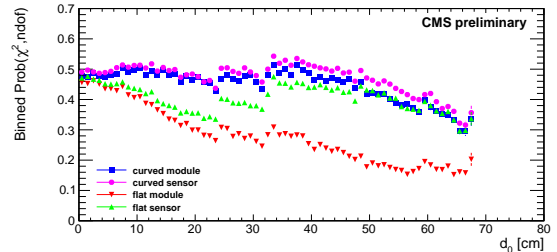


Figure 2: **Distribution of the probability of the χ^2 vs. d_0 (MillePede-II track refit):** For each track the probability of the χ^2 of the MillePede internal track refit for the given number of degrees of freedom is calculated. This plot shows the average per bin, the error bars are the error of the average. The binning is done via the closest distance d_0 of the track to the nominal beamline. Data: Cosmic ray muons, recorded in 2009 during commissioning of CMS. 200 000 tracks used. The results are shown for several cases with different levels of description (see text). At large $d_0 \gtrsim 50$ cm other effects from the track reconstruction start to dominate, which is beyond the normal use-case for the tracker and therefore neglected.

Solving the alignment problem for all these added parameters lead to the determination of roughly 200 000 parameters for the full tracker with Millepede-II in one run. This was performed on a computer equipped with a Intel Nehalem processor and 24 GB of RAM within 6 hours of wall-clock time. Crucial parts of the algorithm were rewritten for multi-threading using OpenMP™ [11] to benefit from parallel processing on the 8 cores the processor offers. The memory consumption for storing the matrix of the normal equations was reduced by using sparse matrix storage schemes and adaptive selection of storage precision of the floating-point numbers at runtime, preserving the required overall precision.

3.1. Estimation of parameter precision

The Gaussian error of the parameters for the bows were estimated using the following observation: When solving for a linear least squares problem on a computer, the crucial step takes place while solving for \mathbf{x} in $\mathbf{M}\mathbf{x} = \mathbf{y}$, \mathbf{M} being the Jacobian matrix of the normal equations. \mathbf{M}^{-1} would be the covariance matrix of the parameters, usually not feasible to solve for as the numerical complexity goes with $O(n^3)$ for matrix inversion, compared to other methods for solving for \mathbf{x} . For this reason, MillePede uses the MINRES algorithm [10] as a solver instead of performing a full inversion. \mathbf{M}^{-1} is therefore not calculated. Individual row vectors \mathbf{M}_i^{-1} of \mathbf{M}^{-1} can be calculated by solving for $\mathbf{M}\mathbf{M}_i^{-1} = \delta_i$, where δ_i is the Kroneckerdelta. This has been carried out, figure 3 shows the results for a part of the pixel barrel detector. The sagittae in the local v direction can be determined to a precision of a few microns. This procedure delivers the statistical error only. No estimate on systematic errors has been carried out yet.

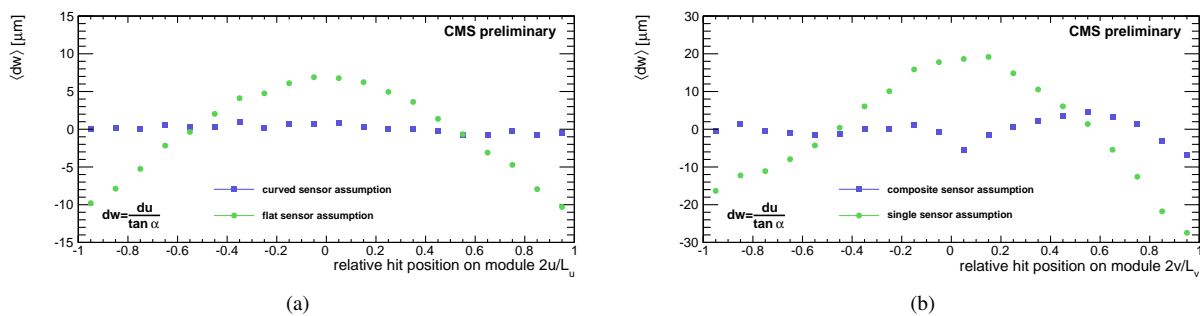


Figure 1: **Residuals perpendicular to surface along modules:** (a) Shown are the observed residuals in the two innermost layers of the strip barrel (tracker inner barrel, TIB), expressed as $dw = du / \tan \alpha$. Green circles: alignment assuming a flat surface. Blue squares: assuming a curved surface (2nd order polynomial in u and v plus mixed term). The measured quantities were the residual du of the measured hit and the position predicted by the track fit, and the track angle α , measured to the normal in direction of u . Only hits fulfilling $|\tan \alpha| > 1/2$ have been used. Results from all modules were used, working on 200 000 cosmic ray tracks. (b) Same shown along v for composite modules in two innermost layers of the tracker barrel with coarser modules (tracker outer barrel, TOB). Green circles: alignment assuming one single flat sensor. Blue squares: assuming two flat sensors, splitted at $2v/L_v = 0$, bows neither determined nor corrected for. Only hits fulfilling $|\tan \alpha| > 1/2$ have been used. Results from all modules were used, working on 200 000 cosmic ray tracks. The splitted surface assumption results in a flatter distribution than the single surface. Observe that in this study there was no correction for the bow, hence the right side shows a bow.

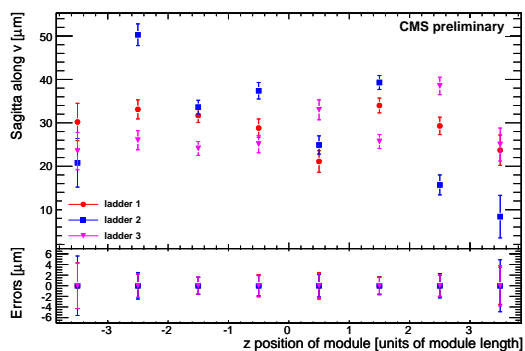


Figure 3: **Error estimate of some parameters (statistical error only):** Shown are the sagittae in v of pixel modules in the innermost layer, determined using a set of collision tracks (1.3 million minimum bias events at $\sqrt{s} = 7$ TeV corresponding to 2.8 million good tracks) and cosmic ray tracks (2.5 million events, corresponding to 1.8 million tracks selected for alignment). The lower part shows the error bars centered at zero.

4. Considerations for future detectors

From the experience of the alignment of a tracking detector at CMS, the following considerations may be helpful in order to enhance the alignability of future detectors of similar design.² We can only speak for the configuration we know, so these thoughts need proper adjustments for other cases and are far from being universal and exhaustive.

Resolution. This seems to be trivial. Two aspects are worth mentioning: The fact that pixels measure two coordinates allows for alignment in all six basic degrees of freedom. Although strips can be aligned in all three rotations, doing so with pixels is far easier. A second important thing is the very high precision of the pitch along one sensor and its constantness on the full area.

²This section reflects the personal suggestions for design considerations for future detectors of one author (*fm*) as given in part at the conference.

Module size. Larger size leads to more hits on one module for a given spatial hit density. This immediately improves the alignment precision by \sqrt{N} . It also improves the determination of angular alignment, as a larger module size translates to a longer lever arm.

Rigid mounting vs. precision mounting. Experiences from CMS show, that certain modules can be aligned even though they are displaced by few mm (sic!) from the design position. If resolution and size are already well chosen, precision mounting does not necessarily help in improving alignment. There might be some configurations for trigger layers, where precision mounting may help for other reasons.

On the other hand, rigid mounting is very important. We understand this as that the modules stay in their position over time. Track-based alignment needs data gathered over long time-periods. As it is averaging in nature, it assumes stability during the time required for recording the data it uses. Movements due to vibrations or imposed by changing conditions like temperature or magnetic field must be slower than the typical data-taking time.

Geometric shape. Barrel-and-endcap configurations have a great advantage for alignment: They deviate sufficiently from an "ideal" sphere-shaped layered detector. The modules are also flat (ore just slightly bowed), which naturally leads to a spread in incident angles on top of what the event topologies may deliver. This helps in creating constraints on several alignment modes.

Tracks from non-standard origin. Such tracks add more constraints on possible movements of modules which are weakly sensitive or even insensitive of changing the χ^2 . Cosmic ray muons are an example in the case of CMS. They come at large d_0 for free whereas in collision data tracks with large d_0 are rare events from secondary vertices. They also may connect parts of the detector with straight tracks which would normally not

270 be connected without imposing special constraints. An exam-321
271 ple for this are the upper and lower hemispheres of a detector,322
272 which are connected with a straight track in the case of cosmic
273 muons. Collision tracks connect these parts as well, but the use
274 of a common-vertex constraint is necessary.323

275 *Optical survey.* Survey has a huge drawback. Usually, survey324
276 is performed under certain artificial conditions before the final325
277 commissioning. It is a, hopefully well established, assumption,326
278 that the survey data stays reliable over time.327

279 Survey is still helpful in several ways. It delivers an independ-328
280 ent knowledge on the geometry at the beginning of the detec-329
281 tors' operation. As the already mentioned tradeoff is present,
282 the investment in survey should be limited. Think of an easy330
283 way of determining the positions of modules. In our case, po-331
284 sition marks from the layer masks used by the manufacturing332
285 process were still visible after mounting. A standard single-333
286 reflex digital camera with a decent macro lens was used to de-334
287 termine relative positions of modules w.r.t their neighbours at a335
288 precision of a few micrometers. Such information can be used336
289 as an independent measurement for validation of the alignment338
290 or it may be treated as independent measurements included in339
291 the alignment algorithm.340

292 *Overlap.* Regions with overlap are useful for alignment and343
293 monitoring of it: Particle tracks have short propagation dis-344
294 tances and therefore their trajectories are less prone to effects345
295 imposed by multiple Coulomb scattering. The short distance346
296 between two sensors along a particle trajectory in regions of347
297 overlap connects them together very tightly.348

298 *Unnecessary features.* In the case of silicon detectors, imple-351
299 menting hardware-based alignment systems is a difficult task.352
300 Either they rely on precision mounting (e.g. some independent353
301 sensors mounted on the frame of the silicon sensors) or they354
302 mimick tracks by using lasers and holes in the metalization.355
303 Only when their precision is at least comparable to the intrin-356
304 sic track hit resolution, a benefit may be realizable. They also
305 may suffer from systematic problems, as their tracks have no
306 geometric spread.

307 *Alignment studies.* The main reason why CMS achieved to
308 align its inner tracker within that short timeframe was the use of
309 well-known algorithms, the work of experienced people and the
310 extensive use of a versatile alignment simulation framework. It
311 is paramount to have the ability to simulate the detector as close
312 to reality as possible before the final construction. There will
313 still be surprises, like the bowed sensors.

314 5. Conclusions

315 The inclusion of a more complex surface description of the
316 silicon sensors of the CMS inner tracker has been shown. This
317 was able to accommodate for discrepancies found in studies on
318 the alignment quality and will improve the track reconstruction
319 in CMS. The sensor bows can be determined with a statisti-
320 cal precision of a few micrometers. We also presented some

thoughts on how future tracking detectors might benefit from
the experience gathered during our work.

6. Acknowledgment

The authors would like to express gratitude to Volker Blobel
for the invention and implementation of the Millepe-II algo-
rithm and the support for it.

The extensions for multithreading and storage optimizations
in Millepede-II was supported by the German Helmholtz Ali-
ance which also maintains the software package[12].

References

- [1] The CMS Collaboration. The CMS experiment at the CERN LHC. *JINST*, 3:S08004, 2008.
- [2] V. Karimäki, A. Heikkinen, T. Lampén and T. Linden. Sensor alignment by tracks paper presented in CHEP03, CHEP-2003-TULT008 <http://arxiv.org/pdf/physics/0306034>
- [3] V. Karimäki, T. Lampén, and F.-P. Schilling. The HIP Algorithm for Track Based Alignment and its Application to the CMS Pixel Detector. CMS Note CMS NOTE-2006/018, CMS collaboration, 2006.
- [4] V. Blobel. Software Alignment for Tracking Detectors. *Nucl. Instr. Methods Phys. Res. A*, 566:5, 2006.
- [5] R. Frühwirth. *Nucl. Instrum. and Methods A*, 262:444 1987.
- [6] A. Strandlie, W Wittek Derivation of Jacobians for the propagation of the covariance matrices of track parameters in homogeneous magnetic fields. *Nucl. Instr. Methods Phys. Res. A*, 566:687 2006.
- [7] V. Blobel A new fast track-fit algorithm based on broken lines. *Nucl. Instr. Methods Phys. Res. A*, 566:14, 2006.
- [8] C. Amsler et al. (Particle Data Group) *Physics Letters B*667, 1 (2008) and 2009 partial update for the 2010 edition
- [9] V. Blobel, C. Kleinwort and F. Meier. Fast alignment of a complex tracking detector using advanced track models. *Submitted to Comp. Phys. Comm.*
- [10] C. C. Paige and M. A. Saunders. Solution of sparse indefinite systems of linear equations *SIAM J. Numer. Anal.* 12(4), 1975, pp. 617-629
- [11] www.openmp.org
- [12] <https://www.wiki.terascale.de/index.php/Millepede-II>, retrieved on Sep 23, 2010.